Machine Learning of Magnetic Phase Transitions

1. Introduction
2. Classical Models of Magnetism
3. Quantum Models of Itinerant Magnetism
4. Conclusions

Wenjian Hu

Natanael Costa

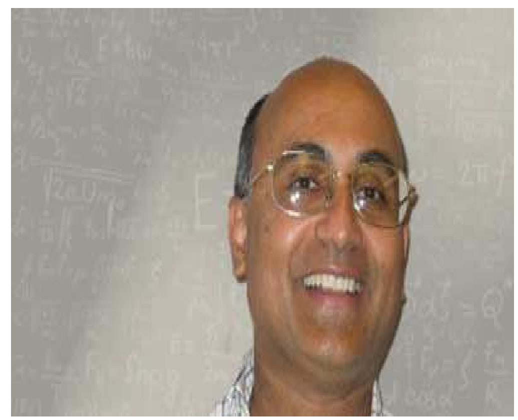

Rajiv Singh

Work supported by NNSA SSAA Program, DE-NA0002908

1. Introduction

Powerful array of existing tools to quantify phase transitions in Monte Carlo:

- Identification of appropriate order parameters.
- Identification of appropriate response functions.
- Finite size scaling.
- Dynamics.

Can require a degree of creativity (even for known order parameter):

- Binder ratio $\langle M^4 \rangle / \langle M^2 \rangle^2$
- Pairing Vertex, $\Gamma = P^{-1} - \bar{P}^{-1}$

Forefront of condensed matter physics today

- Competing types of order

  Cuprates: superconductivity, antiferromagnetism, stripes, nematic, $\cdots$
- More subtle (eg topological) phases.

Develop methods which are useful if the order parameter is not known.

- Recognize novel phases hidden in vast dance of degrees of freedom simulated.

Principal Component Analysis

Basic technical data analysis method of all results presented here.

- P simulations at different parameter values (T, U, ρ).
- L configurations (collection of N degrees of freedom S_j) from each simulation.
- Arrange configurations S_j as row j of a matrix X.
- X is rectangular: PL rows and N columns.
- Construct $\mathcal{M} = X^T X$ (square, dimension N).
- Diagonalize $\mathcal{M}$. Eigenvalues λ_i, "relative variance" $\tilde{\lambda}_i = \lambda_i / \sum_i \lambda_i$
- Inner product of eigenvectors v_i with configurations: $p_{ij} = v_i \cdot S_j$

  "principal components"
- Topology of $\{ (p_{1j}, p_{2j}) \}$ through transition (v_1, v_2: two largest λ_1, λ_2).
- Quantified principal components: $\mathcal{P}_i = \langle | p_i | \rangle = \sum_j | p_{ij} |$

Remainder of this talk: Results

Phase transitions of classical spin models.

Phase transitions of quantum Hamiltonians (itinerant electrons).

2. Classical Models of Magnetism

(i) Ising Model $\quad E = -J \sum_{\langle ij \rangle} S_i S_j \quad S_i = \pm 1$

[See also L. Wang, PRB94, 195105 (2016);
J. Liu, Y. Qi, Z.Y. Meng and L. Fu, PRB95, 041101 (2017)]

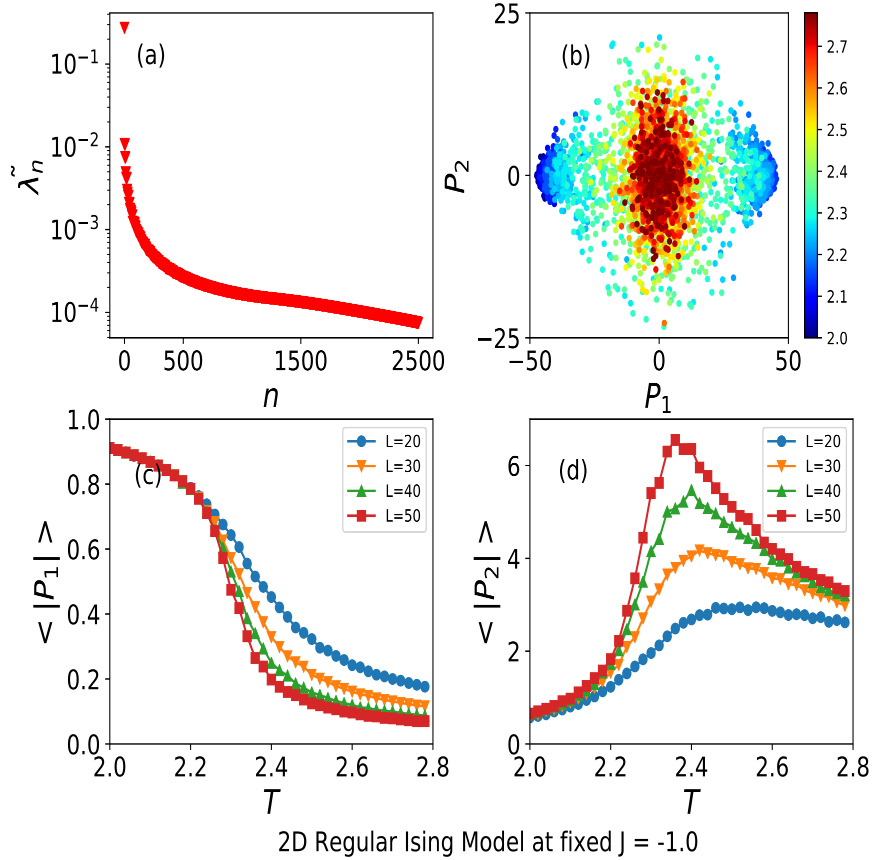

(a) Relative variances $\tilde{\lambda}_i$ drop rapidly with i

(b) $\{ (p_{1j}, p_{2j}) \}$ changes topology at $T_c \sim 2.269$. bifurcates $\rightarrow$ 2 clusters.

(c) $\mathcal{P}_1$ mimics $\langle |M| \rangle$.

(d) $\mathcal{P}_2$ mimics χ.

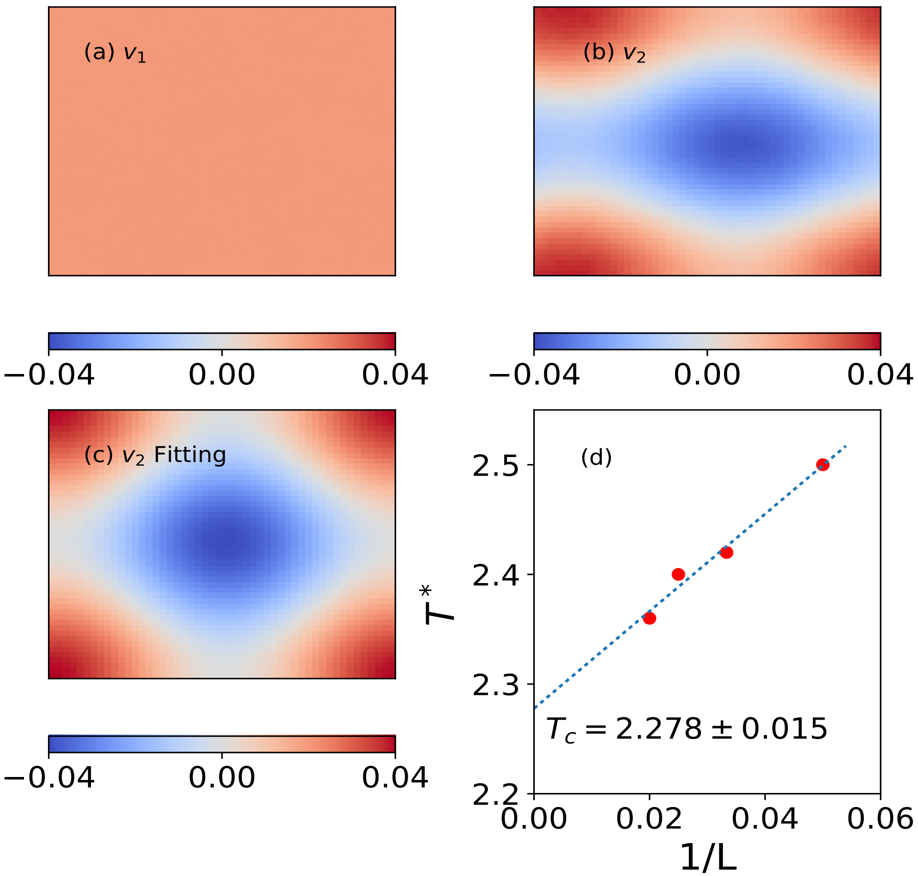

2D Regular Ising Model at fixed J = -1.0

(a) Leading eigenvector v_1 uniform (ferromagnetic).

(b) Subleading eigenvector v_2 domain walls.

(c) Compare to $v_2' = \big(\cos(r_1 k_1), \cos(r_2 k_1), \cdots\big) + \big(\cos(r_1 k_2), \cos(r_2 k_2), \cdots\big)$ $k_1 = (2\pi/L, 0)$, $k_1 = (0, 2\pi/L)$

(d) Extrapolate peaks $T*$ of $\mathcal{P}_2(T)$ with $1/L$.

(ii) Blume-Capel Model $\quad E = -J\sum_{\langle ij\rangle} S_i S_j + \Delta \sum_i S_i^2 \quad S_i = 0, \pm 1$

Ising Model in limit $\Delta \to -\infty$

Tricritical point at $(T/J, \Delta/J) \sim (0.61, 1.97)$

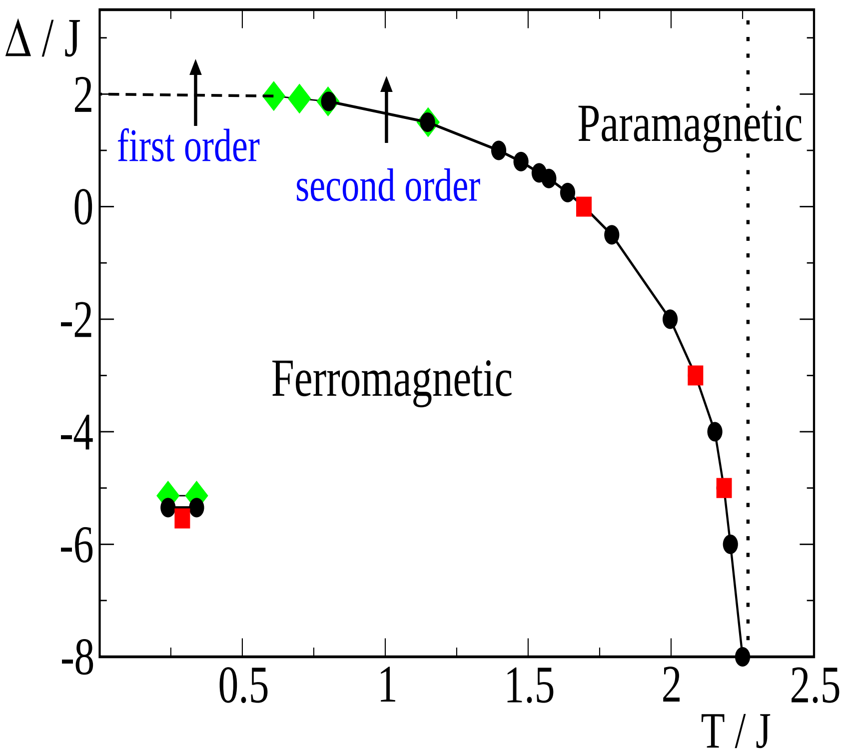

(ii) Blume-Capel Model in second order regime, $T = 1.0$.

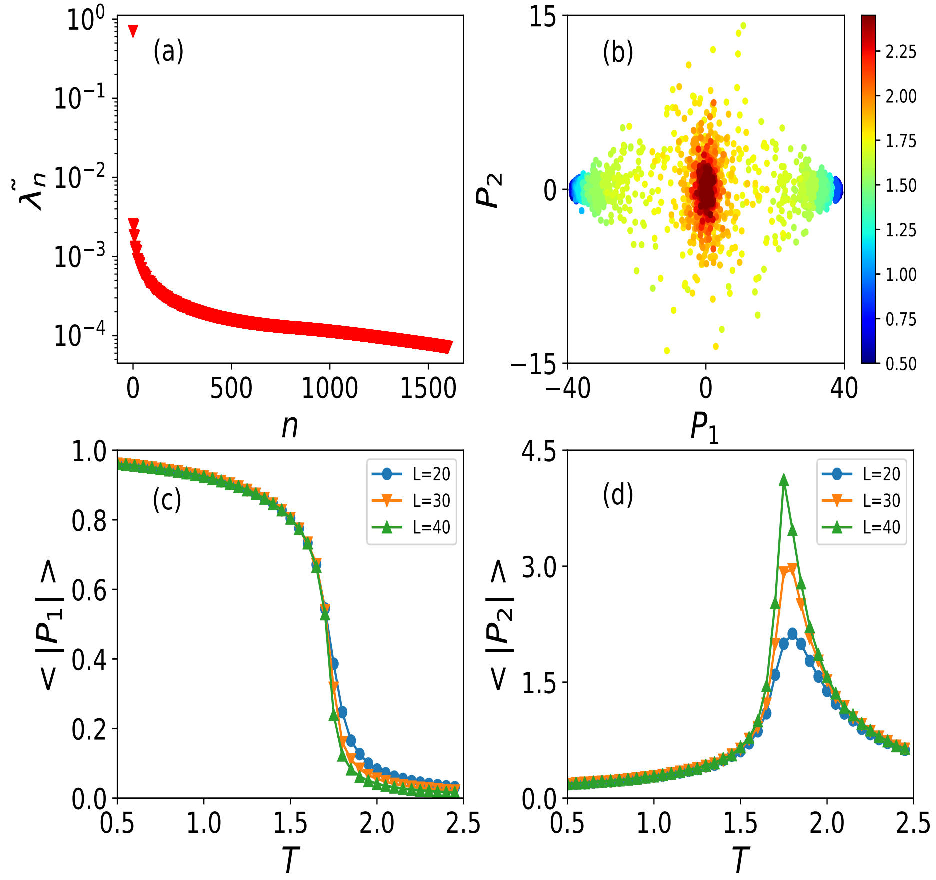

Blume Caple at fixed J=1.0, T=1.0

(a) Relative variances $\tilde{\lambda}_i$ drop rapidly with i

(b) $\{ (p_{1j}, p_{2j}) \}$ changes topology at $\Delta_c \sim 1.7$. 2 cluster bifurcation.

(c) $\mathcal{P}_1$ mimics $\langle \mid M \mid \rangle$.

(d) $\mathcal{P}_2$ mimics χ.

(ii) Blume-Capel Model in first order regime, $T = 0.3$.

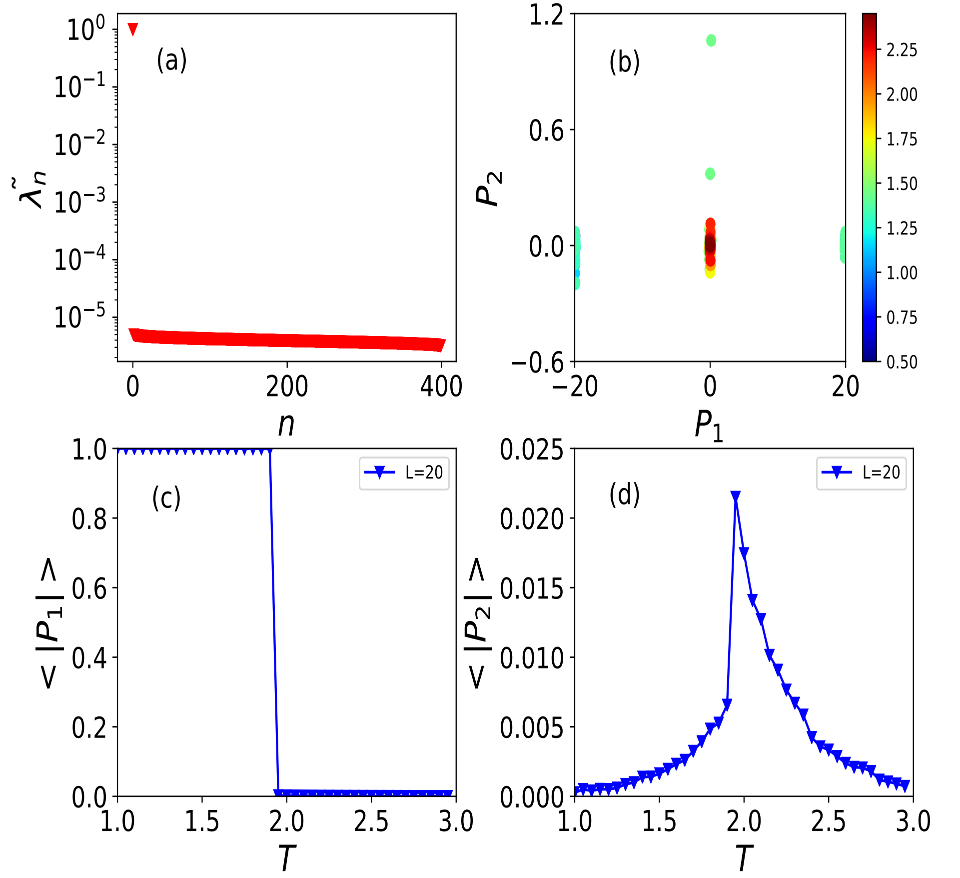

Blume Caple at fixed J=1.0, T=0.3

(a) Relative variances $\tilde{\lambda}_i$ drop rapidly with i

(b) $\{ (p_{1j}, p_{2j}) \}$ changes topology at $\Delta_c \sim 2.0$.

(c) $\mathcal{P}_1$ mimics $\langle \mid M \mid \rangle$.

(d) $\mathcal{P}_2$ mimics χ.

First order character is evident!

(iii) Triangular Lattice Ising Model

No long range order at $T = 0$ (power law spin-spin correlations).

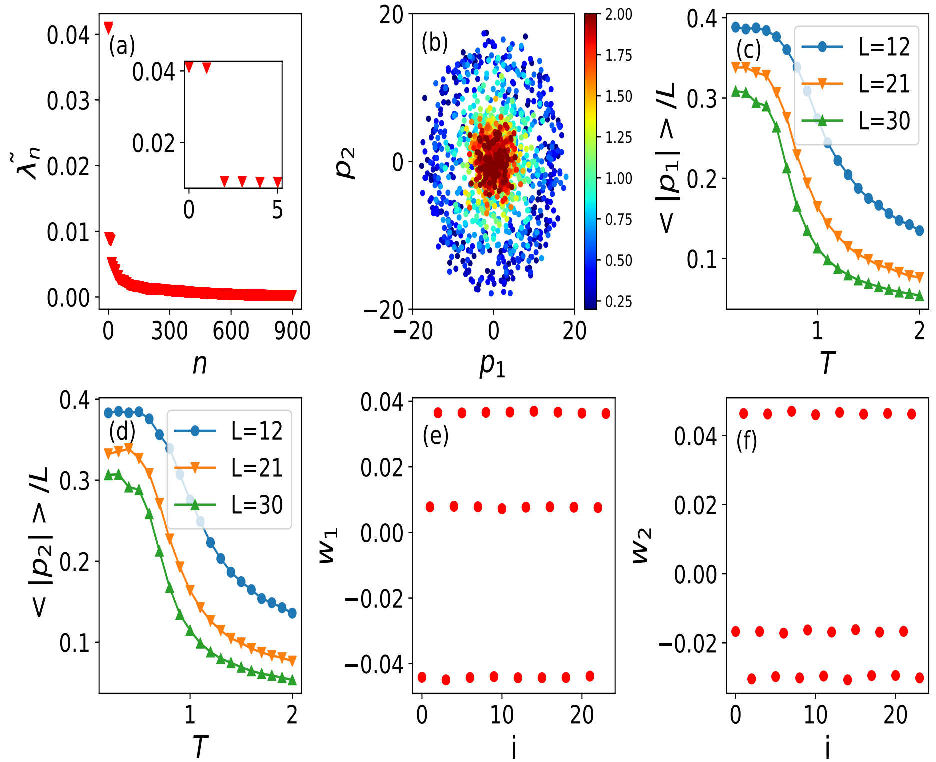

(a) *Pair* of large variances $\tilde{\lambda}_i$

(b) High and low T scatter points separate.

(c,d) Growth of $\mathcal{P}_1$, $\mathcal{P}_2$.

(e,f) Ordering patterns: $(m, 0, -m)$; $(m, -m/2, -m/2)$

These patterns emerge with

- weak transverse field.
- weak interlayer coupling.

PCA recognizes "incipient ordering"!

(iv) Biquadratic Exchange Spin One Ising

$$E = -J \sum_{\langle\langle ik \rangle\rangle} S_i \, S_k + K \sum_{\langle ij \rangle} S_i^2 \, S_j^2 \qquad S_i = 0, \pm 1$$

$K > 0$: Energetically unfavorable $\langle ij \rangle$ both occupied ($S_i = \pm 1$).

- Occupied sites surrounded by vacancies.
- However no preferred spin orientation.

  One sublattice empty ($S_i = 0$).

  Other sublattice *each* site two choices: $S_i = \pm 1$.
- Similar issues to Ising square ice (Carrasquilla)?

Challenge to machine learning:

- Large ground state degeneracy.
- Does a phase transition occur?

(iv) $E = -J\sum_{\langle\langle ik\rangle\rangle} S_i\, S_k + K\sum_{\langle ij\rangle} S_i^2\, S_j^2$

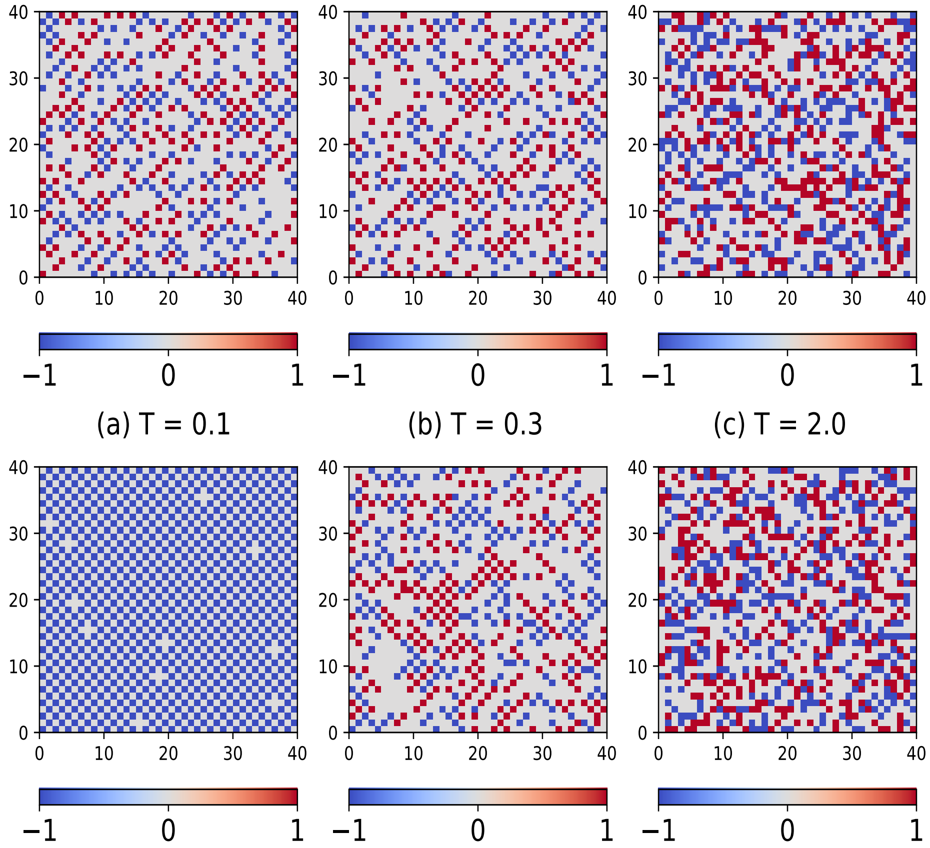

(a) T = 0.1 (b) T = 0.3 (c) T = 2.0

(d) T = 0.1 (e) T = 0.3 (f) T = 2.0

Model not well-studied.
Conventional Monte Carlo.

Spin config snapshots
Top(bottom): $J = 0.0\,(0.1)$
High, intermediate, low T.

$T \sim K$ occupied sites
surrounded by empties.

Order does not emerge $J = 0.0$.

Confirm with $C, S, \langle M\rangle, \chi$.

(iv) Biquadratic Exchange Spin One Ising

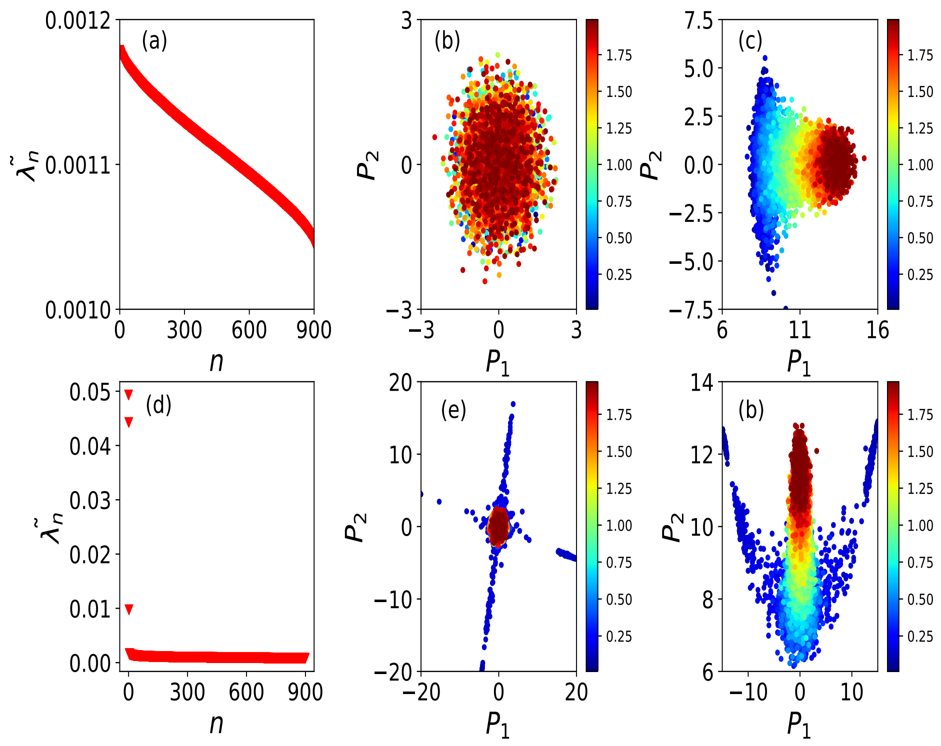

2D Modified Ising Model 3

Top row: $J = 0.0$

(a) Relative variances

- No dominant $\tilde{\lambda}_i$.

(b) $\{\,(p_{1j}, p_{2j})\,\}$

- No hint of ordering.

(c) $\{\,(p'_{1j}, p'_{2j})\,\}$
projections of *squares* of spin configurations exhibit structure but no symmetry breaking (bifurcation in scatter plot).

Model exhibits only gradual crossover at $J = 0.0$.

(iv) Biquadratic Exchange Spin One Ising

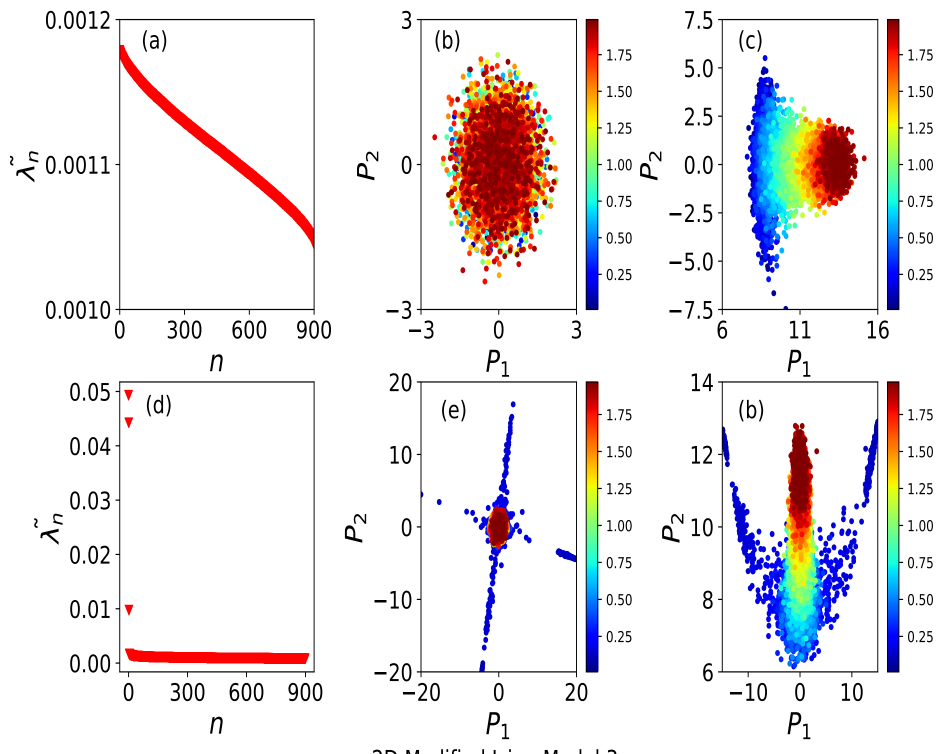

2D Modified Ising Model 3

Bottom row: $J = 0.1$

(a) Relative variances
Dominant $\tilde{\lambda}_i$ emerges.

(b) $\{\, (p_{1j}, p_{2j})\, \}$
Recognize four-fold 'spin' symmetry of ground state.

(c) $\{\, (p'_{1j}, p'_{2j})\, \}$
Recognize two-fold 'charge' symmetry of ground state.

Dominant variance N_v related to ground state degeneracy: $N_g = 2^{N_v}$.

(v) XY Model $E = -J\sum_{\langle ij\rangle}\cos(\theta_i - \theta_j)$

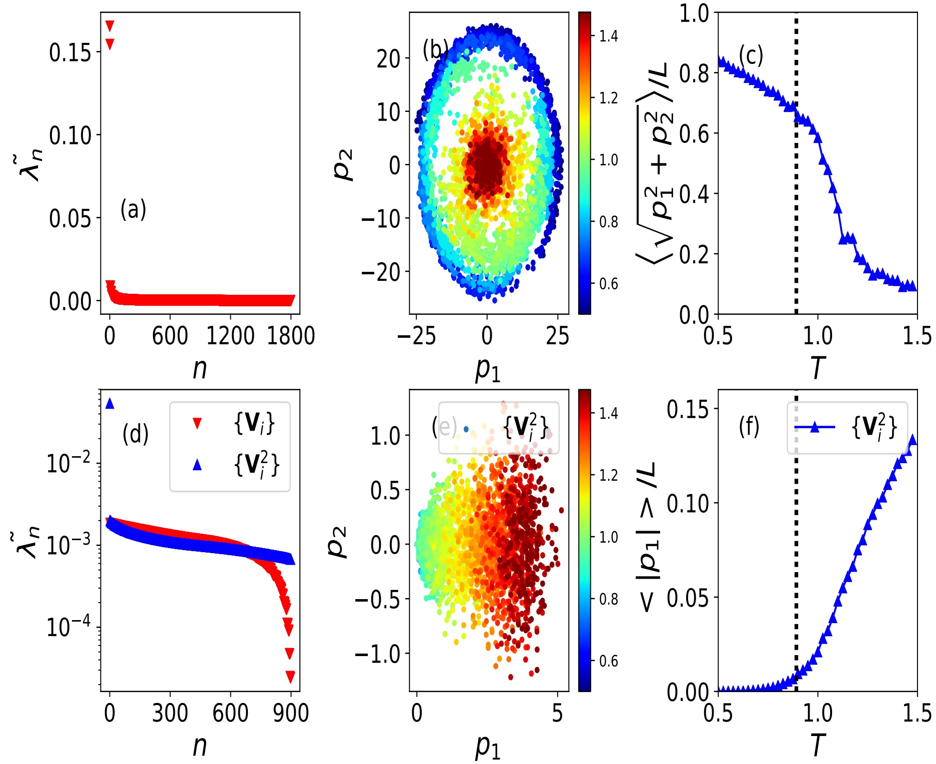

Top:

Feed $(\cos\theta, \sin\theta)$ into PCA.

(a) Two equally weighted relative variances.

(b) Principle components occupy periphery of circle at low T.

(c) $\sqrt{\mathcal{P}_1^2 + \mathcal{P}_2^2}$ shows signal near $T_{KT} \sim 0.892$.

(v) XY Model $\quad E = -J\sum_{\langle ij\rangle}\cos(\theta_i - \theta_j)$

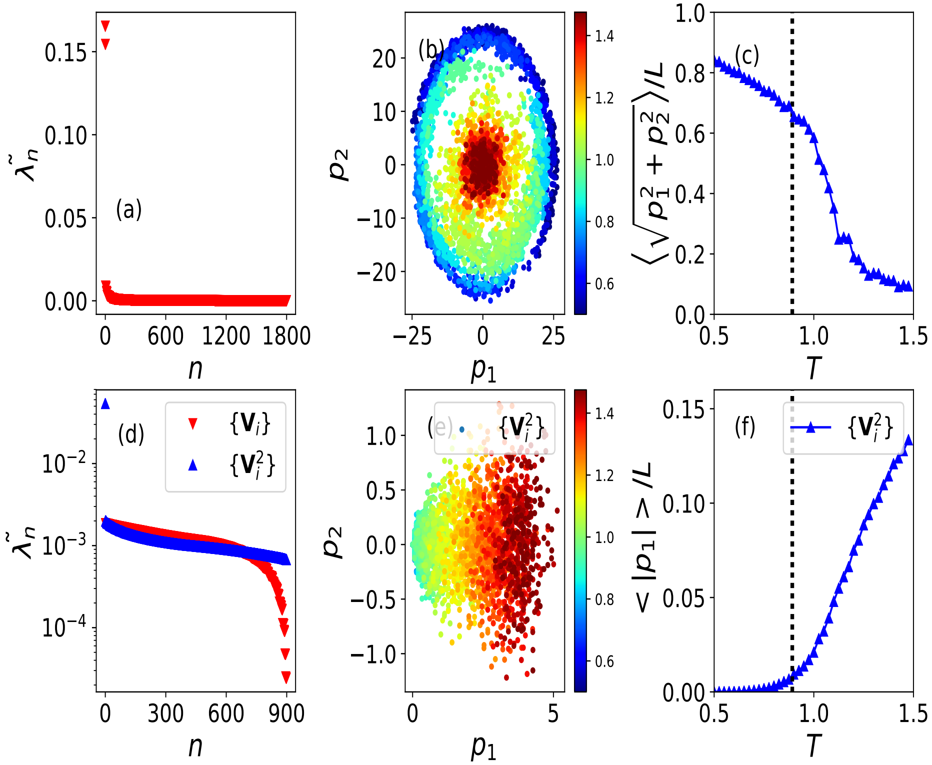

Bottom:

Local vorticity V_i into PCA.
(d) No dominant λ_i (red).

Local vorticity square V_i^2
(d) Dominant $\tilde{\lambda}_i$ (blue).

(e,f) Principle components evolve in smooth crossover.

Vortex binding-unbinding may be challenging for machine learning.

3. Quantum Models of Magnetism

Methodology is determinant Quantum Monte Carlo (DQMC).

Electron-electron interactions decoupled via introduction of discrete 'Hubbard-Stratonovich' field $S_{i\tau}$.

$S_{i\tau}$ has spatial $i = 1, 2, \cdots N$; imaginary time $\tau = 1, 2, \cdots L$ indices.

$L = \beta/\Delta\tau$: number of divisions of inverse temperature.

Options for PCA:

- Provide $S_{i\tau}$ for all i at single τ, or all τ at single i.
- Provide $S_{i\tau}$ for all i, τ.
- Provide (vorticity in XY), a 'derived quantity': e.g. Greens function.

Prior work (very partial list!):

Xiao Yan Xu, Yang Qi, Junwei Liu, Liang Fu, Zi Yang Meng, arXiv:1612.03804.

K. Ch'ng, J. Carrasquilla, R.G. Melko, and E. Khatami, arXiv:1609.02552v2.

P. Broecker, J. Carrasquilla, R.G. Melko, and S. Trebst, arXiv:1608.0784v1.

(Q-i) Hubbard Model on honeycomb lattice.

$$\hat{H} = -t \sum_{\langle ij \rangle \sigma} \left(c_{i\sigma}^{\dagger} c_{j\sigma} + c_{j\sigma}^{\dagger} c_{i\sigma} \right) + U \sum_{i} n_{i\uparrow} n_{i\downarrow}$$

Honeycomb lattice, half-filling: AF order if $U > U_c \sim 3.8$.

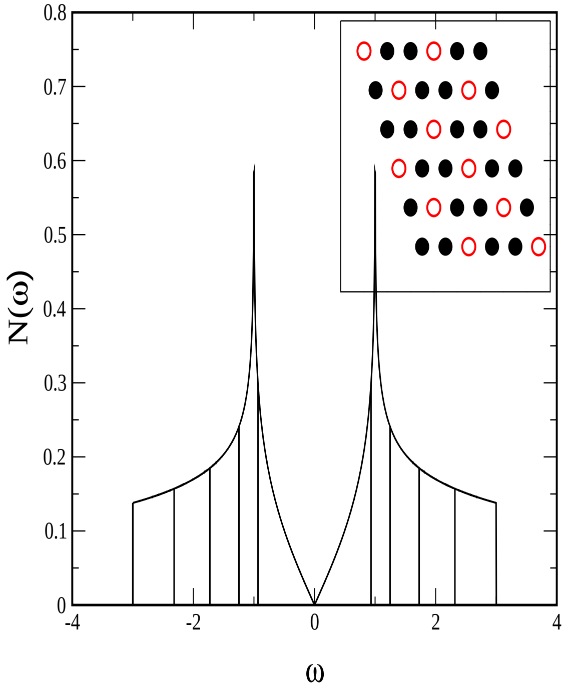

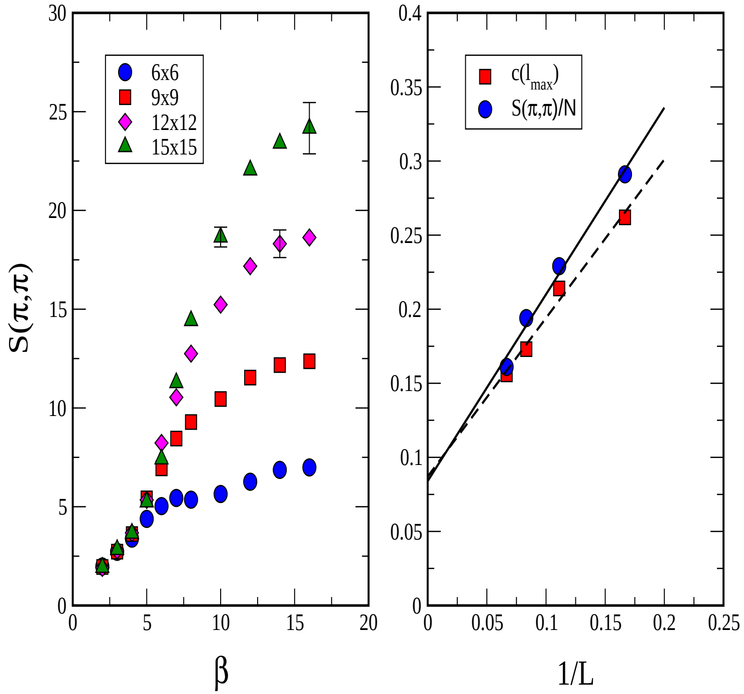

(Q-i) Hubbard Model on honeycomb lattice.

$$\hat{H} = -t \sum_{\langle ij \rangle \sigma} \left(c_{i\sigma}^{\dagger} c_{j\sigma} + c_{j\sigma}^{\dagger} c_{i\sigma} \right) + U \sum_{i} n_{i\uparrow} n_{i\downarrow}$$

Honeycomb lattice, half-filling: AF order if $U > U_c \sim 3.8$.

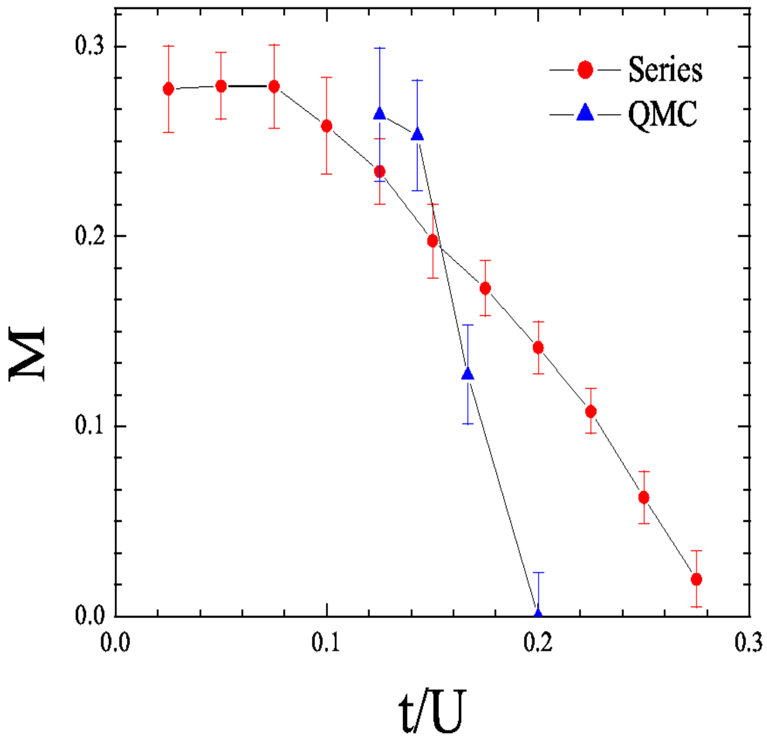

(Q-i) Hubbard Model on Honeycomb lattice.

$\hat{H} = -t \sum_{\langle ij \rangle \sigma} \left(c^{\dagger}_{i\sigma} c_{j\sigma} + c^{\dagger}_{j\sigma} c_{i\sigma} \right) + U \sum_i n_{i\uparrow} n_{i\downarrow}$

Honeycomb lattice, half-filling: AF order if $U > U_c \sim 3.8$.

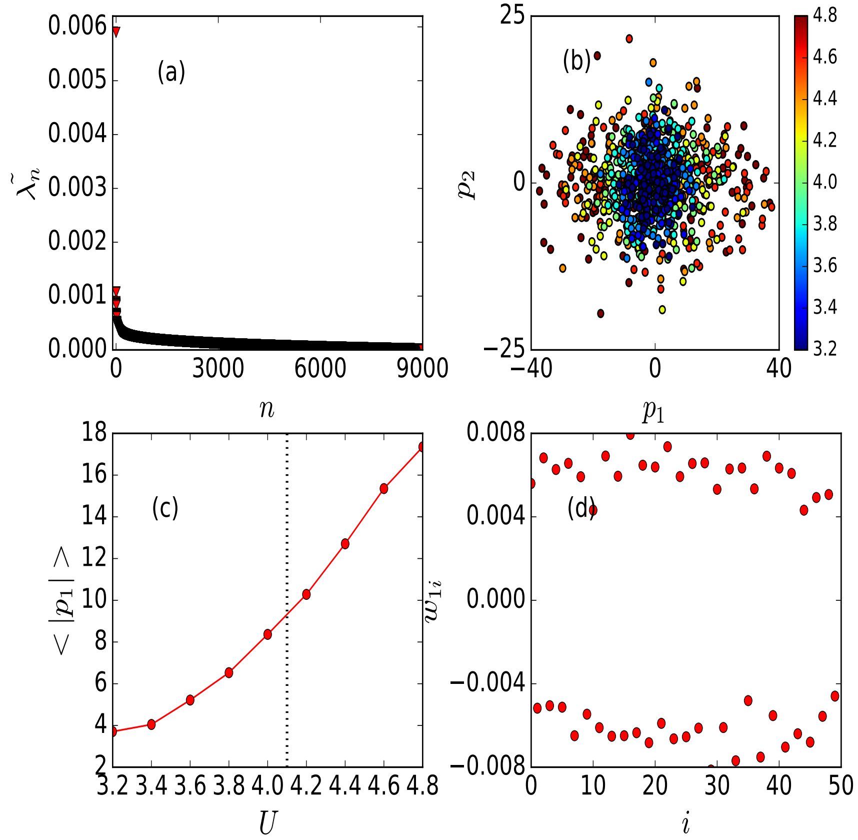

(a) Dominant variance $\tilde{\lambda}_i$

(b) Central $(\mathcal{P}_1, \mathcal{P}_2)$ peak bifurcates as U increases.

(c) Principal component AF pattern.

(Q-ii) Periodic Anderson Model

$$\hat{H} = -t \sum_{\langle ij \rangle \sigma} \left(d^{\dagger}_{i\sigma} d_{j\sigma} + d^{\dagger}_{j\sigma} d_{i\sigma} \right) + U^f \sum_i n^f_{i\uparrow} n^f_{i\downarrow} + V \sum_{i\sigma} \left(f^{\dagger}_{i\sigma} d_{i\sigma} + d^{\dagger}_{i\sigma} f_{i\sigma} \right)$$

Antiferromagnetic $\rightarrow$ singlet transition, $V > V_c \sim 1.18$ for $U^f = 6$.

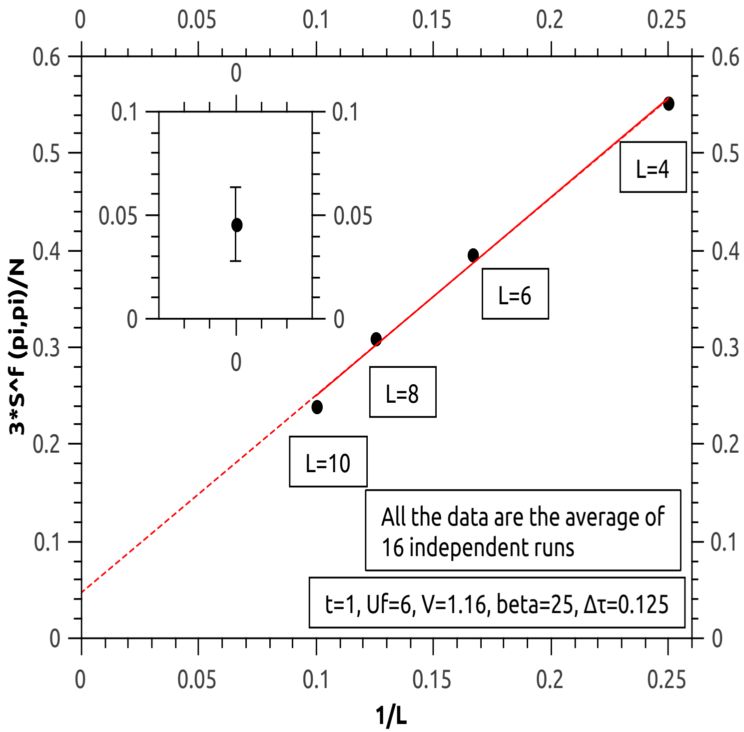

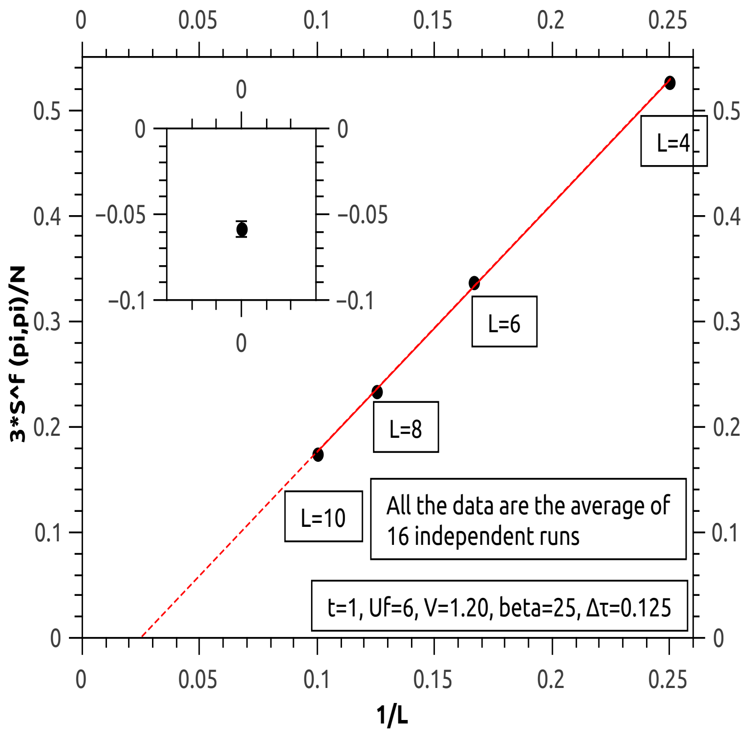

(Q-ii) Periodic Anderson Model

$$\hat{H} = -t \sum_{\langle ij \rangle \sigma} \left(d^\dagger_{i\sigma} d_{j\sigma} + d^\dagger_{j\sigma} d_{i\sigma} \right) + U^f \sum_i n^f_{i\uparrow} n^f_{i\downarrow} + V \sum_{i\sigma} \left(f^\dagger_{i\sigma} d_{i\sigma} + d^\dagger_{i\sigma} f_{i\sigma} \right)$$

Antiferromagnetic $\rightarrow$ singlet transition, $V > V_c \sim 0.99$ for $U^f = 4$.

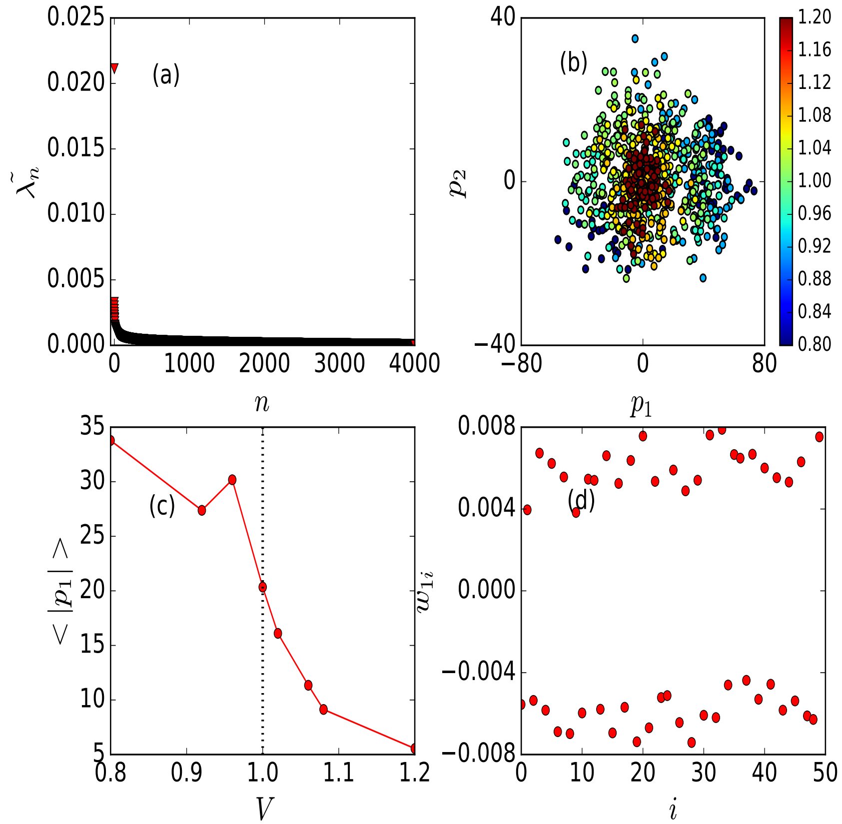

(a) Dominant variance $\tilde{\lambda}_i$

(b) Central $(\mathcal{P}_1, \mathcal{P}_2)$ peak collapses as V increases.

(c) Principal component AF pattern.

(Q-iii) Hubbard Model on Lieb Lattice

Three bands: two dispersing, bracket flat band.

Ferrimagnetic order at half-filling.

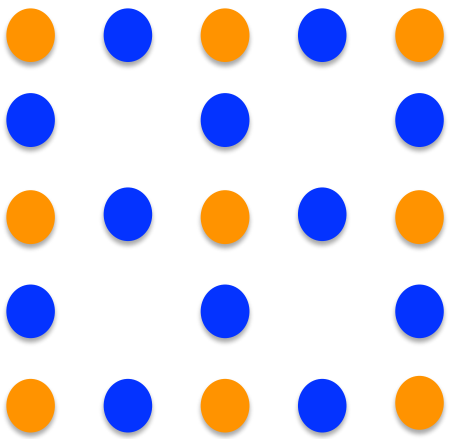

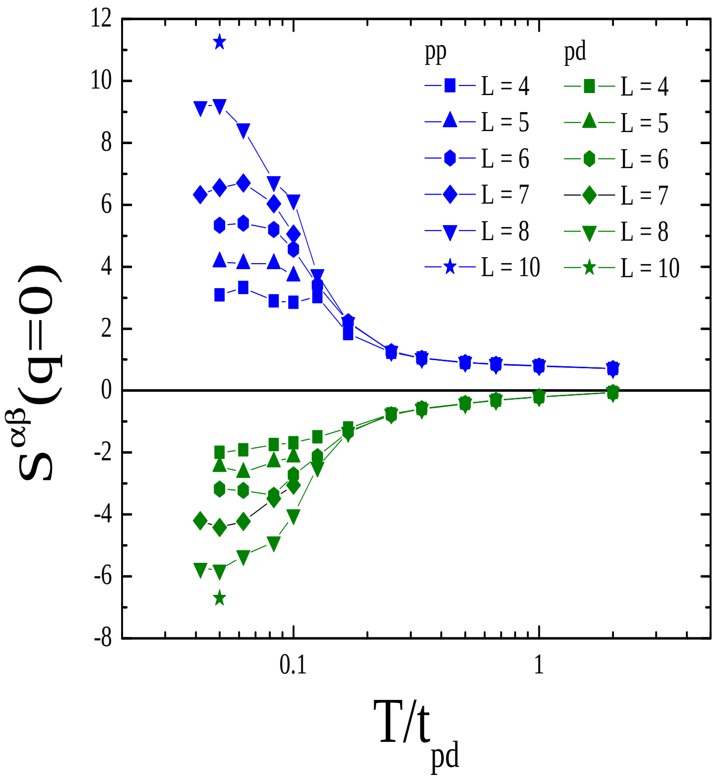

(Q-iii) Hubbard Model on Lieb Lattice

Three bands: two dispersing, bracket flat band.

Half-filling of lowest band ($\rho = 1/3$) AF order.

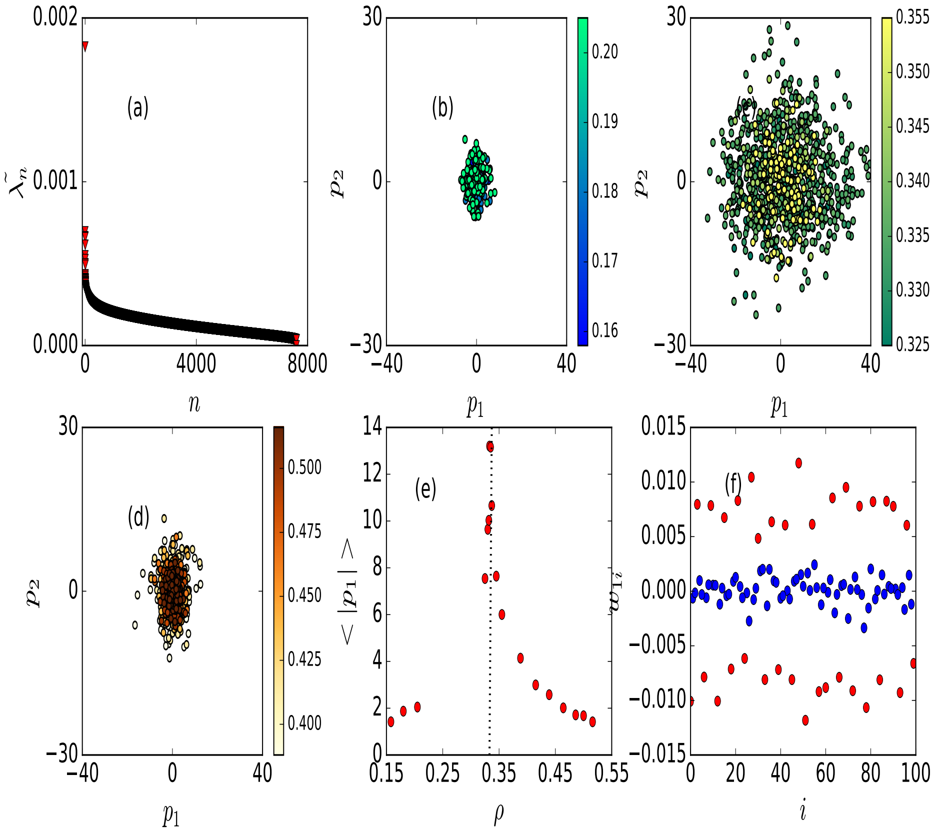

(a) Dominant variance $\tilde{\lambda}_i$

(b,d) Central $(\mathcal{P}_1, \mathcal{P}_2)$ peak

(c) expanded $\rho \sim 1/3$.

(e) $\mathcal{P}_1$ peak at $\rho = 1/3$.

(f) AF pattern (bridge sites).

PCA for doped system

(weak sign problem).

(Q-v) Holstein model: e^- coupled to phonons: $S_{i\tau} \to x_{i\tau}$.

$$\hat{H} = -t \sum_{\langle ij \rangle \sigma} \left(c^\dagger_{i\sigma} c_{j\sigma} + c^\dagger_{j\sigma} c_{i\sigma} \right) + \frac{1}{2} \sum_i \left(p_i^2 + \omega^2 x_i^2 \right) + g \sum_i x_i \left(a^\dagger_i + a_i \right)$$

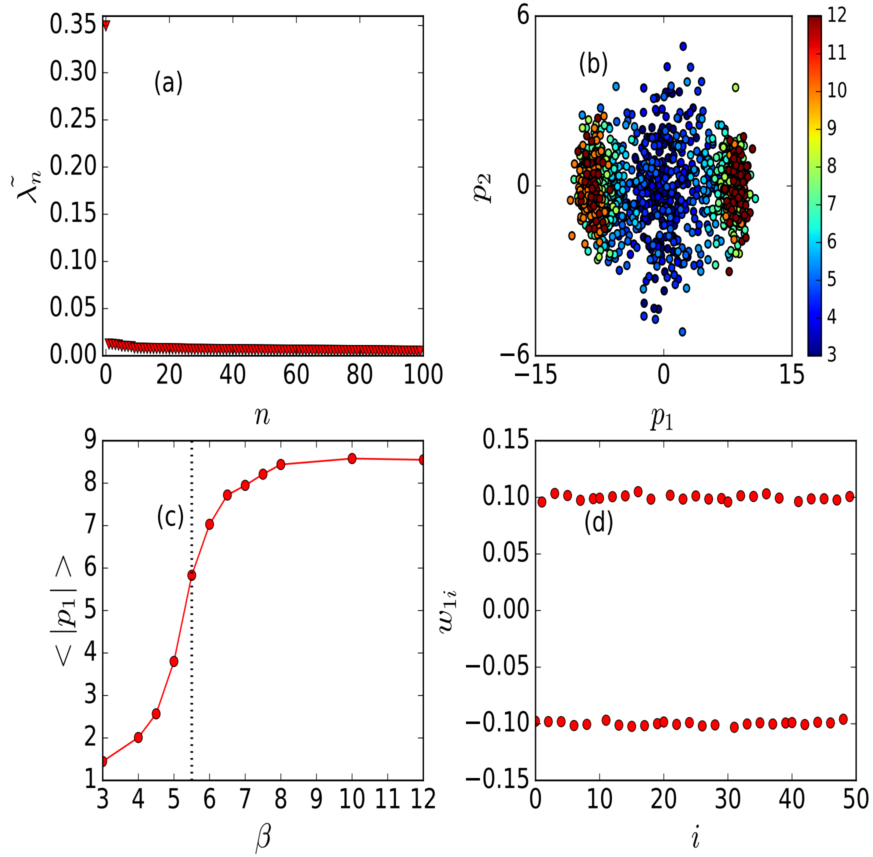

Half-filling: Simultaneous CDW and SC order at $T = 0$.

Doped: SC transition of KT type (these results). $\beta_c \sim 8$.

(a) Dominant variance $\tilde{\lambda}_i$

(b) $(\mathcal{P}_1, \mathcal{P}_2)$ divides at low T.

(c) $\mathcal{P}_1$ order onset $\beta \sim 6$.

(d) Remnant CDW order.

4. Conclusions

Primitive machine learning method (PCA) can discern phase transitions.

Ising and Blume-Capel

- Dominant principle component $\leftrightarrow$ order parameter;
- Recognizes symmetry breaking; first vs second order transitions.
- Sub-dominant principle components: small q behavior (domain walls).

Triangular lattice Ising, Biquadratic Spin, XY

- PCA on frustrated models (highly degenerate ground states);
- Bring out subtle incipient order.
- Cannot recognize order in $S_i^2(V_i^2)$ from only $S_i(V_i)$.

PCA is useful for discerning quantum magnetism and charge order.

Can machine learning methods beat 'traditional' approaches ?!